Chemical Engineering Journal 179 (2012) 1–7

Contents lists available at ScienceDirect

Chemical Engineering Journal

journal homepage: www.elsevier.com/locate/cej

Pretreatment of wastewater from acrylonitrile–butadiene–styrene (ABS) resin manufacturing by microelectrolysis

Bo Lai[a,b], Yuexi Zhou[a,*], Hongke Qin[a], Changyong Wu[a], Cuicui Pang[a,c], Yu Lian[a,c], Jixian Xu[c]

[a] Research Center of Water Pollution Control Technology, Chinese Research Academy of Environment Sciences, Beijing 100012, China
[b] College of Water Sciences, Beijing Normal University, Beijing 100875, China
[c] College of Urban Construction, Hebei University of Engineering, Handan, Hebei 056038, China

ARTICLE INFO

Article history:
Received 13 October 2010
Received in revised form
10 December 2010
Accepted 29 December 2010

Keywords:
Microeletrolysis
ABS resin wastewater
Aromatic compounds
Organic nitriles

ABSTRACT

Pretreatment of acrylonitrile–butadiene–styrene (ABS) resin wastewater by microelectrolysis system was investigated to improve the biodegradability of the toxic aromatic compounds and organic nitriles. Two experiment systems, (a) control experiment of Fe and carbon and (b) microelectrolysis reactor, were set up to confirm the importance of macroscopic galvanic cells. In addition, the effect of the influent pH and Fe/C ratio on the efficiency of the microelectrolysis reactor was studied. The experimental results showed that the maximum COD removal efficiency was in the range of 50–55%, and the BOD_5/COD ratio was enhanced from 0.32 to 0.71 under the best condition of the influent pH 4 and Fe/C ration of 1:1 (*v*/*v*). The microelectrolysis reactor could not remove the nitrogen in ABS resin wastewater, but it could transform the organic nitriles into NH_3-N, amine and acylamide, and the NH_3-N transformation efficiency reached 50% when the influent pH was 4. The decomposition and transformation of the aromatic compounds and organic nitriles in ABS resin wastewater was monitored by UV–vis, fourier transform infrared spectroscopy (FTIR) and gas chromatography mass spectrometry (GC–MS). This study showed that an almost total decomposition or transformation of the toxic organic pollutants and an increasing biodegradability of the pretreated ABS resin wastewater could be achieved by microelectrolysis reactor.

1. Introduction

In China, most of the acrylonitrile–butadiene–styrene (ABS) resin plants use emulsion grafting-blend production method to produce various types of ABS resin [1]. With this production method, styrene, acrylonitrile and hundreds of auxiliary agents are needed in the entire production process, which leads to a toxic, refractory and complicated ABS resin wastewater [2]. If the untreated wastewater is discharged into the receiving water directly, it will cause serious environmental problems. In literature, it is hard for conventional biological processes to mineralize all typical pollutants of ABS resin wastewater, especially for low polymer, and microbial activity would be inhibited by some toxic substance such as the aromatic compounds and organic nitriles [3–6]. Ozone oxidize method and photocatalysis oxidation of modified nano TiO_2 have been used for the pretreatment of ABS resin wastewater [7,8], while other potential technologies such as fenton reagent, three-dimensional electrode reactor and wet air oxidation can also be used to treat this wastewater [9–11]. However, all of these pretreatment methods suffer the limitations of high costs. So it is necessary to discover and develop an effective, robust and economically feasible pretreatment method for ABS resin wastewater.

Since the microelectrolysis was discovered and first applied in printing and dyeing wastewaters in 1970s, this technology has widely used in the preatreatment of industrial wastewaters such as petrochemical wastewater, acrylic fiber wastewater, olive mill wastewater, electroplating wastewater and pharmaceutical wastewater [12–16]. Iron chips and activated carbon are commonly used as electrolytic materials of microelectrolysis. When a mixture of iron chips and activated carbon is in contact with wastewater (electrolyte solution), numerous macroscopic galvanic cells are formed between the particles of iron and carbon, and numerous microscopic galvanic cells are also formed in interior of iron chips because of cementite. The electrons are supplied from the galvanic corrosion of iron (anode) [12], and the half-cell reactions can be represented as:

$$\text{Anode(oxidation)}: Fe - 2e^- \rightarrow Fe^{2+} \quad E^{\theta}(Fe^{2+}/Fe) = -0.44\,V \quad (1)$$

$$\text{Cathode(reduction)}: \text{acidic}: 2H^+ + 2e^- \rightarrow 2[H] \rightarrow H_2\uparrow \quad E^{\theta}(H^+/H_2) = 0.00\,V \quad (2)$$

* Corresponding author. Tel.: +86 01084915311; fax: +86 01084915311.
E-mail address: zhouyuexi@263.com (Y. Zhou).

1385-8947/$ – see front matter © 2011 Elsevier B.V. All rights reserved.
doi:10.1016/j.cej.2010.12.089

Table 1
Characteristics of ABS resin wastewater.

Item	Values ($mg\,L^{-1}$)
COD	1100–1300
BOD_5	400–500
TOC	350–450
TN	90–110
TKN	80–100
NH_3-N	5–15

$$\text{Acidwithoxygen}: O_2 + 4H^+ + 4e^- \rightarrow 2H_2O$$
$$E^{\theta}(O_2/OH^-) = 1.23\,V \quad (3)$$

$$\text{Neutraltoalkaline}: O_2 + 2H_2O + 4e^- \rightarrow 4OH^-$$
$$E^{\theta}(O_2/OH^-) = 0.40\,V \quad (4)$$

It is clear that organic pollutants can be oxidized by radicals and oxidants produced from electrode action. Furthermore, organic pollutants can also be reduced by Fe, Fe^{2+} and [H] during microelectrolysis [13]. Additionally, organic pollutants can also be removed by adsorption, enmeshment and coprecipitation by the ferric and ferrous hydroxides formed from oxidation and precipitation of Fe^{2+}. In addition, activated carbon can also adsorb some of the organic pollutants, especially for those hydrophobic ones [12].

The goal of this study is to investigate characteristics of adsorption, enmeshment, coprecipitation and electrochemical action of the microelectrolysis system for ABS resin wastewater. Furthermore, degradation or transformation of the toxic refractory typical pollutants was monitored by UV–vis, FTIR and GC–MS analyses.

2. Materials and methods

2.1. Raw wastewater

The wastewater used in this study was obtained from a petrochemical industry in northern China. The physicochemical characteristics of ABS resin wastewater are listed in Table 1.

2.2. Reactor system

The experimental apparatus was a cylindrical microelectrolysis reactor (Φ10 cm × 50 cm). The reactor was made of transparent synthetic glass column. The granular activated carbon (GAC) and sponge iron were mixed together, and then packed in the reactor as a fixed bed with a bed height of 40 cm.

A commercial granular activated carbon (GAC) from Beijing Ke Cheng Guang Hua New Technology Company was used in this study. It has mean particle size of approximately 5 mm, an electric resistance of about 5 Ω for each activated carbon particles, a specific surface of $748\,m^2\,g^{-1}$ according to the BET method, a total pore volume of $0.481\,mL\,g^{-1}$ and a bulk density of $0.493\,g\,cm^{-3}$. A commercial sponge iron was obtained from Beijing Ming Jian Technology Company. It has mean particle size of approximately 5 mm and a bulk density of $3\,g\,cm^{-3}$. The iron content of the sponge iron reaches 98%.

2.3. Experimental method

Organic pollutants removal during microelectrolysis treatment results from the combined effect of adsorption of GAC [17], coprecipitation and enmeshment of the ferrous and ferric hydroxide floc [12], and electrochemical action of microelectrolysis [12,13]. In order to quantify the electrochemical action occurring during simultaneous physical–chemical processes, two control experiments were set up: (a) GAC without sponge iron in reactor (Control-C), (b) sponge iron without GAC in reactor (Control-Fe). The volume of GAC and sponge iron in control was in accord with that of the microelectrolysis reactor, and the influent pH of the control was 4.0. To investigate the effect of influent pH on organic pollutants removal by the microelectrolysis reactor, pH of the influent was adjusted to 4.0, 6.0 and 8.0 by adding diluted sulfuric acid (10%) or sodium hydroxide solutions ($5\,mol\,L^{-1}$). All of the reactors were operated continuously 30 d with a constant hydraulic retention time (HRT) of 4 h, and measurements were routinely taken of COD, BOD_5, total kjeldahl nitrogen (TKN), NH_3-N, pH, UV–vis, FTIR and GC–MS.

2.4. Analytical methods

Gas chromatography mass spectrometry (GC–MS) was used for organic compounds analysis. Prior to GC–MS determination, a 20 mL sample was extracted using 10 mL CH_2Cl_2 (Chromatogram Pure Grade, Fisher, USA) three times under acidic, neutral and alkaline conditions, respectively. The three extracted layers were mixed, dehydrated with anhydrous sodium sulfate and dried with the aid of a nitrogen flow. The residue was dissolved in 1.0 mL CH_2Cl_2 and 1 μL was injected into a 7890/5975 GC–MS system (Agilent, USA) equipped with a HP-5MS capillary column of inner diameter 0.25 mm and 30.0 m in length. The GC column was operated in temperature programmed mode at 40 °C for 1 min, raised at $20\,°C\,min^{-1}$ to 100 °C, and then raised at 10–280 °C (held for 3 min). The solvent delay was 4 min and the total run time was 25 min. The mass range scanned was 20–700 m/z. Analysis was undertaken with reference to the NIST 05 mass spectral library database.

Fourier transform infrared spectroscopy (FTIR) was used to assess the differences in the general functional groups of the influent and effluent of the two control experiments and microelectrolysis reactor. 300 mg KBr was milled by pestle and mortar, once fine enough the powder was placed in a mould and compressed into a pellet with a force 10 tons applied for 1 min. The pellet was then placed in a holder and scanned using a Perkin Elmer 100 FTIR spectrometer and the background spectra were generated using its software. To obtain the spectra for the influent and effluent, the samples were first dried and grinded, and then each sample (6 mg) was mixed with 300 mg KBr and milled into powder by pestle and mortar. The powder mixture was placed in a mould and compressed into a pellet under10 tons force for 1 min. Each sample was scanned four times between the wavelengths 4000 and $400\,cm^{-1}$.

The UV–vis absorption spectrum of the ABS resin wastewater was carried out in 10 mm quartz cuvettes, and the UV–vis spectra were recorded from 190 to 350 nm using deionized water as blank. Optical micrographs were obtained with an optical microscope (BX-51, Olympus, Japan). The chemical oxygen demand (COD) and biochemical oxygen demand (BOD_5) were determined using a COD analyzer (Hach, USA) and respirometer (OxiTop IS12, WTW, Germany), respectively. The total kjeldahl nitrogen (TKN) was determined by a kjeldahl nitrogen apparatus (KDY-9830, Ketuo, China). Ammonia nitrogen (NH_3-N) of the samples was determined according to standard methods [18] and pH was measured by a pHS-3C meter (Rex, China).

3. Results and discussion

3.1. Effect of influent pH and Fe/C ratio on COD removal efficiency and biodegradability

Fig. 1 illustrated the COD removal of ABS resin wastewater in microelectrolysis reactors at different Fe/C ratios (v/v). The results

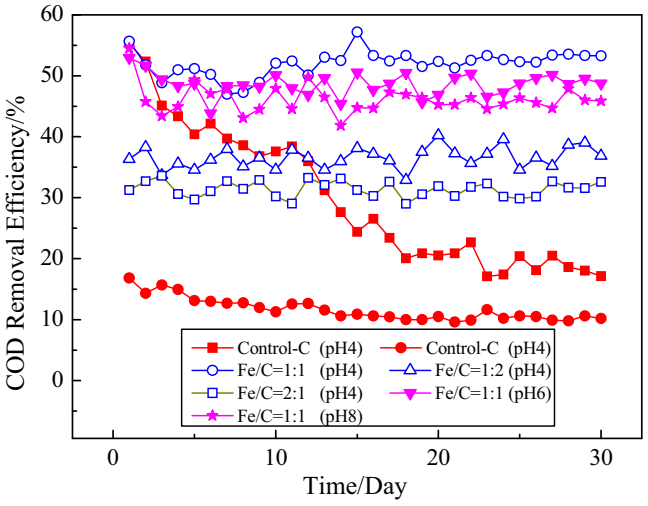

Fig. 1. Effect of influent pH and Fe/C ratio on COD removal efficiency.

suggested that the removal efficiency was the highest with Fe/C ratio of 1:1 (*v*/*v*). The same volume of Fe and C in reactor means the same anode and cathode number, which is in favor of the formation of macroscopic galvanic cells. Therefore, the ratio of 1:1 (*v*/*v*) for Fe/C was selected in the following studies.

The curve of control experiment (carbon) shows that COD removal efficiency decreases quickly to 55% after the first day, and then decreases gradually from 55 to 20% in the initial 18 d, finally, it remains between 17 and 22% in the following days. The results of control experiment (carbon) suggest that the removal of organic pollutants is mainly resulted from the adsorption of GAC in the initial stage, and the constant COD removal efficiency in the latter stage is resulted from numerous filamentous microorganisms (as shown in Fig. 2) which are domesticated under the acidic and anaerobic conditions. It has been reported that the filamentous microorganisms can degrade the aromatic compounds [19,20], and there are plenty of aromatic compounds in ABS resin wastewater (as shown in Table 2). Therefore, the constant COD removal efficiency (17–22%) of control experiment (carbon) is caused by the degradation of the aromatic compounds in ABS resin wastewater by filamentous microorganisms. However, those filamentous microorganisms were not observed in other reactors, which resulted from the effect of electrochemistry action or high concentration ferrous and ferric ion. Therefore, in the microelectrolysis reactors and control experiment of Fe, the COD of ABS resin wastewater is mainly removed through physics adsorption, co-precipitation, enmeshment and electrochemical action.

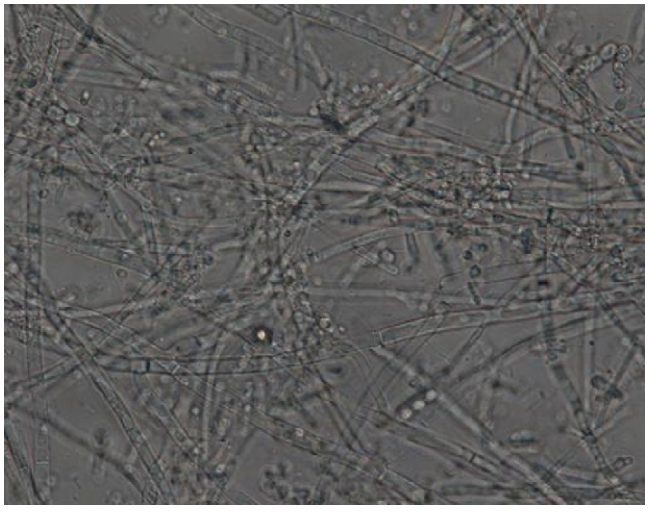

Fig. 2. Optical micrograph of filamentous microorganisms in control experiment carbon (400×).

The curve of control experiment of Fe shows that the COD removal efficiency remains approximate 10% in the entire 30 d, which resulted from microscopic galvanic cells of sponge iron and the co-precipitation and enmeshment of the ferrous and ferric hydroxide floc. The sponge iron contains many impurity particles, such as Fe_3C and C, and these very small particles are dispersed in the matrix of sponge iron, which form thousands of microscopic galvanic cells with iron. However, only the microscopic galvanic cells on the surface of sponge iron can contact the wastewater and degrade the pollutants, so their COD removal efficiency is very low. In addition, it is clear that the co-precipitation and enmeshment of the ferrous and ferric hydroxide floc also cannot remove the organic pollutants in ABS resin wastewater directly. Therefore, the control experiment of Fe can only degrade a little part of organic pollutants in ABS resin wastewater.

Fig. 1 shows that the COD removal efficiencies of three microelectrolysis reactors with different influent pH in sequence are as follow: pH = 4 > pH = 6 > pH = 8. The influent pH is an important parameter affecting the kinetics in the pretreatment process. Different reaction rates are obtained for the reaction of zero-valent iron in ABS resin wastewater with different pH, which are presented as following equations:

$$Fe + 2H^+ \rightarrow Fe^{2+} + H_2 \quad (5)$$

$$Fe + 2H_2O \rightarrow Fe^{2+} + H_2 + 2OH^- \quad (6)$$

According to Nernst Equation, the reaction rate of $Fe \rightarrow Fe^{2+}$ increases with an increase of the H^+ concentration, therefore the pretreatment efficiency of microelectrolysis system can be affected by the influent pH. It is clear that COD removal efficiency of the microelectrolysis reactor is about four times than that of the control experiment of Fe which only has microscopic galvanic cells. The microelectrolysis reactor has microscopic and macroscopic galvanic cells, and the number of macroscopic galvanic cells is much larger than that of microscopic galvanic cells. Therefore, the macroscopic galvanic cells play a major role in the COD removal. Moreover, the macroscopic galvanic cells may convert the complex organic contaminants into the aromatic by-products with carboxyl functional groups (e.g., benzoic acid), which are expected to bind strongly to ferrous and ferric hydroxide floc [12]. In other words, the organic contaminants in ABS resin wastewater can be removed indirectly by co-precipitation and enmeshment of the ferrous and ferric hydroxide floc.

In this experiment, the biodegradability of the influent and effluent of control experiments and microelectrolysis reactors was monitored by measuring the BOD_5/COD ratio. Fig. 3 shows that the BOD_5/COD ratios of the effluent of different reactors are all higher than those of the influent, and the BOD_5/COD ratios of the effluent of the three microelectrolysis reactors are much higher than those of the two control experiments. These imply that the macroscopic galvanic cells play a leading role in the degradation of toxic refractory organic pollutants and improvement of biodegradability for ABS resin wastewater. Fig. 3 shows that the BOD_5/COD ratios of the effluent of three microelectrolysis reactors with different influent pH in sequence are as follow: pH = 4 > pH = 6 > pH = 8. This indicates that the influent pH affect the improvement of biodegradability for ABS resin wastewater.

Regarding above results, it can be concluded that the microelectrolysis reactor cannot only remove the COD of this wastewater efficiently but also improve its biodegradability significantly, which mainly attributed to the macroscopic galvanic cells. Besides, the COD removal efficiency and BOD_5/COD ratio of the effluent of the

Table 2
Main organic compounds analysis of ABS resin wastewater.

Retention time (min)	Organic compounds	Proposed structures	Area percentage (%)	Main fragment
(1) 4.54	3-Dimethylaminopropanonitrile	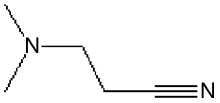	4.62	58(100%), 42, 30, 15
(2) 4.68	Styrene	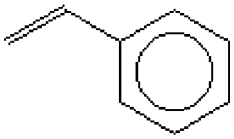	2.43	104(100%), 78, 51, 41, 31
(3) 6.88	3-Diethylaminopropiononitrile	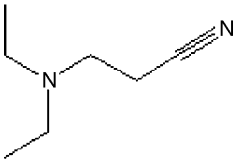	0.92	111(100%), 86, 58, 42, 28
(4) 7.35	Acetophenone	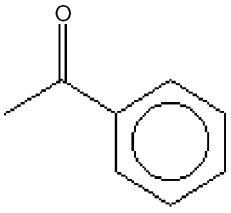	10.72	120, 105 (100%), 77, 51
(5) 7.72	α,α-Dimethylbenzenemethanol	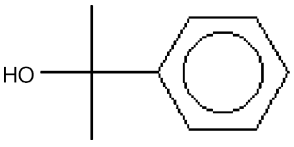	42.16	121, 91, 77, 51, 43(100%)
(6) 10.52	3,3-Oxydipropionitrile	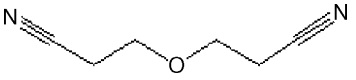	13.03	84, 54(100%), 40, 28
(7) 11.63	3,3′-Iminodipropionitrile	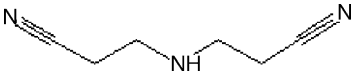	19.86	83(100%), 54, 42, 28
(8) 13.13	3,3′-Thiodipropionitrile	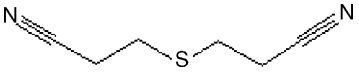	3.75	140, 100, 54(100%), 45

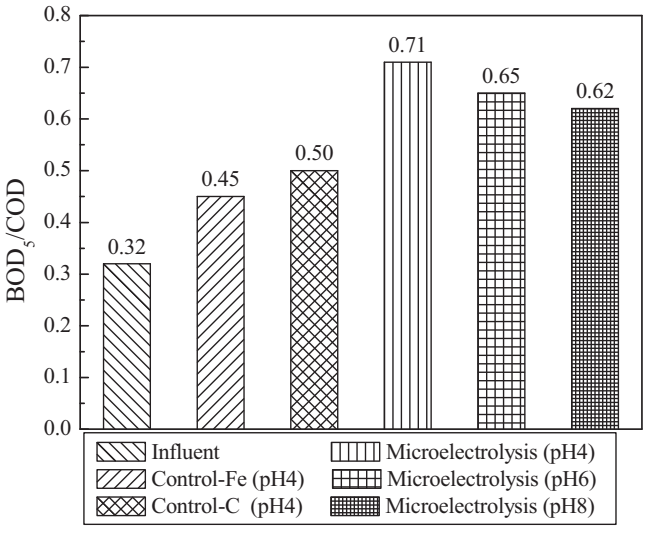

Fig. 3. BOD_5/COD of the influent and effluent of the two control experiment and three microelectrolysis reactors with different influent pH.

microelectrolysis reactor increase with the decreasing of influent pH, and the best influent pH of the microelectrolysis reactor is about 4.

3.2. UV–vis spectral changes

After 30 d run, the changes in UV–vis absorbance characteristics of the influent and effluent of the microelectrolysis reactor and two control experiments from 190 to 350 nm are shown in Fig. 4. The absorbance peak at the wavelength of about 230 nm can be assigned to the π–π^* transition of benzene rings [21–23] such as acetophenone and α,α-dimethylbenzenemethanol (as shown in Table 2), respectively. The absorbance peak at the wavelength of about 200 nm can be attributed to the combination of the nitrile group of the organic nitriles and the benzene ring of monoaromatics. The main organic nitriles of ABS resin wastewater are 3-dimethylaminopropanonitrile, 3-diethylaminopropiononitrile, 3,3-oxydipropionitrile, 3,3′-iminodipropionitrile and 3,3′-thiodipropionitrile (as shown in Table 2), which contained non-conjugated C(N and auxochrome group (e.g., –NR, –OR). Therefore, the absorbance peak

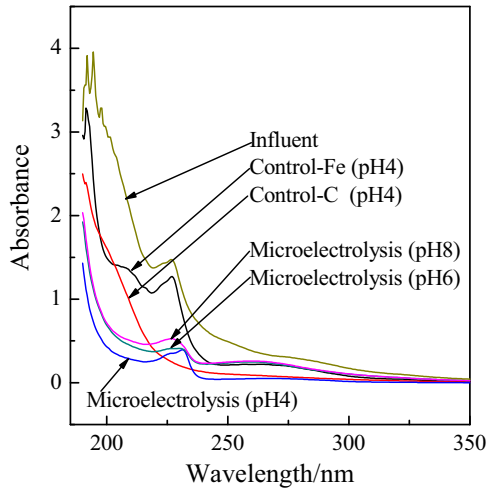

Fig. 4. UV–vis spectra of the influent and effluent of the two control experiment and three microelectrolysis reactors with different influent pH.

of the organic nitriles is at the wavelength of about 200 nm [21].

As shown in Fig. 4, the absorbance of the effluent of control experiment (Fe) is only dropped a little with respect to the influent, which is a clear sign that the control experiment (Fe) can only degrade a little part of the aromatic compounds and organic nitriles in ABS resin wastewater. The absorbance peak at the wavelength of about 230 nm is dropped significantly after the treatment of control experiment (carbon), while the absorbance peak at the wavelength of about 200 nm was only dropped a little. It can be concluded that the control experiment (carbon) can only degrade the aromatic pollutants. All peaks of UV–vis spectra for the effluent of microelectrolysis reactors decreased strongly. However, there remained a little peak at the wavelength of about 235 nm for the effluent, which indicated that some by-products containing benzoic-type rings (e.g., benzoic acid) might be produced after the decomposition and transformation of the aromatic pollutants [24,25].

3.3. Decomposition and transformation of nitrogen

Fig. 5(a) shows that there is dependence of TKN removal efficiencies on running time under the condition of influent pH 4. Fig. 5(a) shows that the TKN removal efficiencies of the two control experiments were both dropped below 10% after the first day, and then remained below 5% in the following days. This suggests that the activated carbon and sponge iron cannot adsorb or remove the TKN of ABS resin wastewater significantly. However, the TKN removal efficiency of the microelectrolysis reactor dropped gradually from 35 to 5% in the initial 15 d, and then remained below 5% in the latter. The higher TKN removal efficiency of the microelectrolysis reactor in the initial stage is probably caused by the adsorption of the by-products (e.g., amine, acylamide) associated with transformation of the organic nitriles in ABS resin wastewater. These by-products are much easier to be adsorbed by activated carbon or ferrous and ferric hydroxide floc compared to the organic nitriles of ABS resin wastewater. Therefore, the higher TKN removal efficiency in initial stage is due to the adsorption of nitrogen-containing by-products, while the gradual decrease of TKN removal efficiency with treatment time is associated with the adsorption saturation of activated carbon. In a word, the microelectrolysis reactor cannot remove the nitrogen of ABS resin wastewater, but it can transform the organic nitrogen.

Fig. 5(b) shows that there is dependence of NH_3-N transformation efficiencies on running time under the condition of influent pH 4. The NH_3-N transformation efficiency (NH_3-N%) is determined according to the following equation:

$$(NH_3\text{-N})\% = \frac{C^n_{NH_3\text{-N}} - C^\circ_{NH_3\text{-N}}}{C^\circ_{TKN} - C^\circ_{NH_3\text{-N}}} \times 100\% \quad (7)$$

where $C^\circ_{NH_3\text{-N}}$ and $C^n_{NH_3\text{-N}}$ are the ammonia–nitrogen concentrations of the influent and effluent at the nth day, respectively. C°_{TKN} is the TKN concentration of the initial. Fig. 5(b) shows that the NH_3-N transformation efficiency of the control experiment (carbon) is 0% in the entire 30 d, which indicates that the filamentous microorganisms cannot decompose and transform the organic nitriles in ABS resin wastewater. The NH_3-N transformation efficiency of the control experiment (Fe) was increased from 0 to 14% in the initial 5 d, and then remained between 13 and 17%. The NH_3-N transformation efficiency of the microelectrolysis reactor increased gradually from 1 to 53% in the initial 10 d, and then remained between 50 and 55% in the latter. It is clear that the NH_3-N transformation efficiency of microelectrolysis reactor is much higher compared to that of control experiment (Fe), which implies that the macroscopic galvanic cells play a leading role in decomposition and transformation of the organic nitriles in ABS resin wastewater. The gradual increase of the NH_3-N transformation efficiency of the microelectrolysis reactor in the initial stage reveals that the NH_3-N can be adsorbed by activated carbon or ferrous and ferric hydroside floc which will reach their maximum adsorption capacity in the initial 10 d.

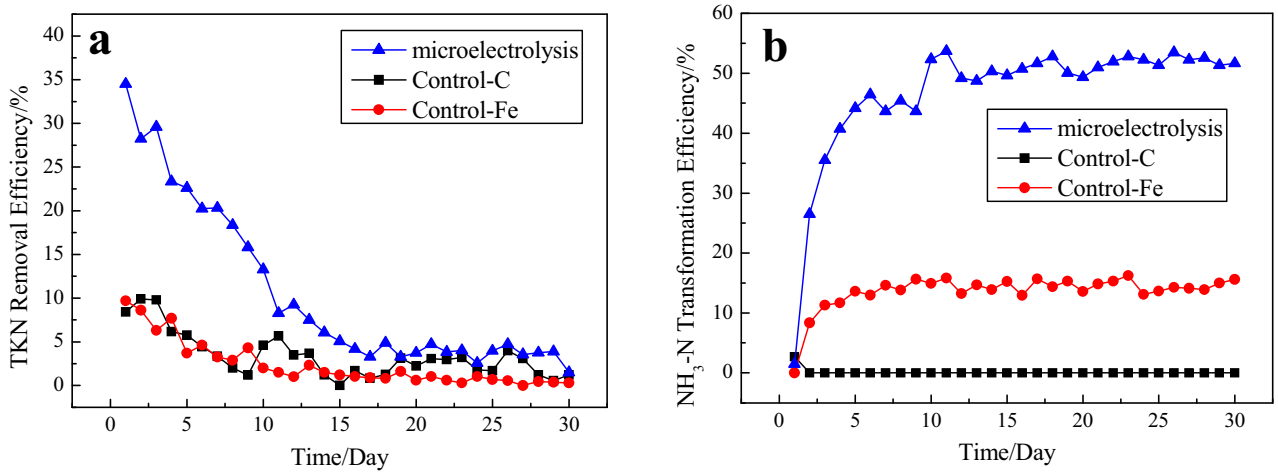

Fig. 5. Change of the nitrogen of ABS resin wastewater in the 30 d.

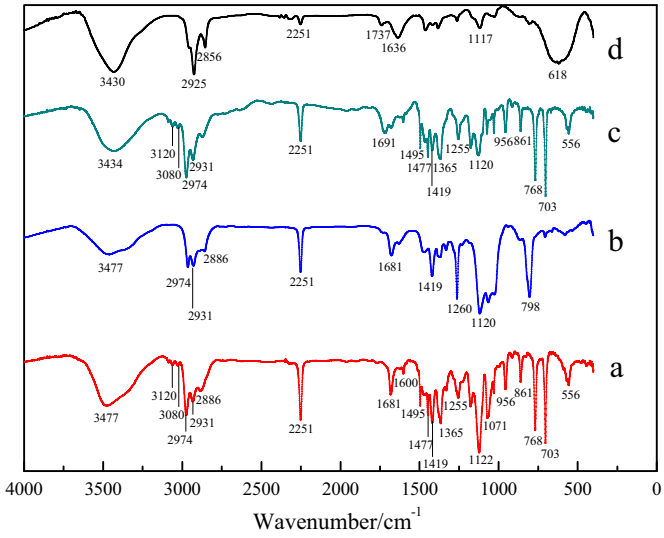

Fig. 6. FTIR adsorption spectra of the 400–4000 cm^{-1} region of influent and effluent: (a) influent, (b) control-carbon, (c) control-Fe, (d) microelectrolysis reactor.

3.4. FTIR adsorption spectra analysis

After the 30 d run, the four FTIR adsorption spectra of the influent and effluent of the electroelectrolysis reactor and two control experiments are illustrated in Fig. 6(a)–(d), respectively. The absorbance bands are interpreted by information from prior reports [26–29].

Fig. 6(a) is the FTIR adsorption spectrum of the influent of the electroelectrolysis reactor and two control experiments. The band at 3477 cm^{-1} is attributed to the overlap of O–H stretching, N–H stretching and hydrogen-bonded OH; the bands at 3080 and 3120 cm^{-1} are attributed to stretching of aromatic C–H; the bands at 2886, 2931 and 2974 cm^{-1} are attributed to the stretching of CH_2 group; the band at 2251 cm^{-1} is attributed to the C(N stretching in fatty nitriles; the band at 1681 cm^{-1} is attributed to C=O of H-bonded conjugated ketones and/or quinones; the bands at 1447, 1495 and 1600 cm^{-1} are attributed to the aromatic C=C skeletal vibrations; the band at 1419 cm^{-1} is attributed to the C–N stretching. It is implied that the main organic compounds of the crude ABS resin wastewater are aromatic compounds, fatty nitriles and organic amines. Therefore, the results of FTIR spectra are mainly consistent with the results of GC–MS analysis (as shown in Fig. 7 and Table 2).

Fig. 6(b) is the FTIR adsorption spectrum of the effluent of the control experiment (carbon). This spectrum shows all the peaks of the influent except the aromatic peaks at 3080 and 3120 cm^{-1} (stretching of aromatic C–H), 1447, 1495 and 1600 cm^{-1} (the aromatic C=C skeletal vibrations). These can be attributed to the decomposition and transformation of the aromatic compounds by filamentous microorganisms.

Fig. 6(c) is the FTIR adsorption spectrum of the effluent of the control experiment (Fe). This spectrum shows all the peaks of the influent, but their peak intensity is a little lower compared to that of the influent. That is caused by the weaker degradation capacity of control experiment (Fe) which only had microscopic galvanic cells. In other words, the control experiment (Fe) can only degrade and transform a little part of organic pollutants in ABS resin wastewater.

Fig. 6(d) is the FTIR adsorption spectrum of the effluent of the microelectrolysis reactor with influent pH 4. All the peaks of the influent disappeared except the peaks at 3430 cm^{-1} (the overlap of O–H stretching), 2856 and 2925 cm^{-1} (the stretching of CH_2 group). These confirm that the microelectrolysis reactor with macroscopic galvanic cells can decompose and transform all the aromatic compounds and the organic nitriles in ABS resin wastewater. Moreover, several new peaks at 1117 cm^{-1} (C–O stretching of secondary alcohols), 1636 cm^{-1} (C=O stretching in amides I, ketones, acids or quinones), 1737 cm^{-1} (C=O stretching in carboxyls, acids and ketones), 618 cm^{-1} (N–H, O–N=O) are observed in the effluent of the microelectrolysis reactor. It is clear that some by-products (e.g., carboxylic acid, ketone, amine, amide) are produced after the decomposition of the aromatic compounds and organic nitriles in ABS resin wastewater.

Regarding above results, we can conclude that the microelectrolysis reactor can transform the toxic organic pollutants in ABS resin wastewater into less toxic by-products, and the macroscopic galvanic cells of the microelectrolysis reactor play a leading role in the degradation of toxic organic pollutants.

3.5. GC–MS analysis

In this experiment, the biodegradability of treated ABS resin wastewater is monitored by measuring the BOD_5/COD ratio. The effluent is considered as biodegradable when the BOD_5/COD ratio

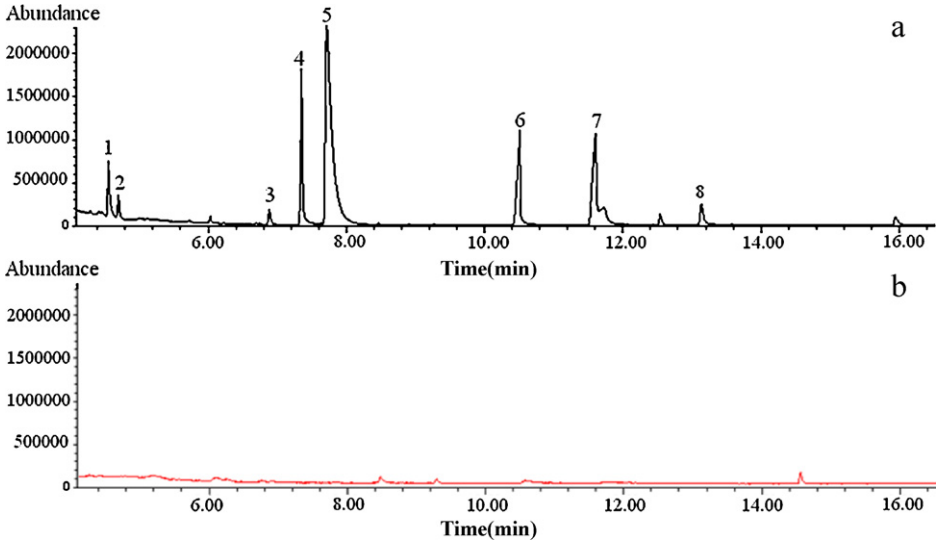

Fig. 7. GC–MS chromatograms on dichloromethane extract from (a) influent and (b) effluent of the microelectrolysis reactor with influent pH 4.

is higher than 0.4. Regarding BOD_5/COD ratio which is equal to 0.32, it is clear that the crude ABS resin wastewater is toxic and refractory. Fig. 3 shows that the BOD_5/COD ratio of ABS resin wastewater is raised from 0.32 to 0.71 after the treatment of microelectrolysis reactor with influent pH 4, which indicated the high biodegradability of the wastewater. This proves that the microelectrolysis reactor is efficient to enhance the biodegradability of this toxic wastewater.

The improvement of the biodegradability of ABS resin wastewater can be explained by the decomposition or transformation of the aromatic compounds and organic nitriles by microelectrolysis reactor. This is confirmed by GC–MS analysis of the influent and effluent of microelectrolysis reactor. In fact, the two chromatograms of the influent and effluent are represented in Fig. 7(a) and (b). According to Fig. 7(a), three aromatic compounds (55.31%) and five organic nitriles (42.18%) can be identified in crude ABS resin wastewater, and these compounds are summarized in Table 2. By comparison, the chromatogram of Fig. 7(b) does not present any aromatic compounds or organic nitriles, which suggests that the microelectrolysis reactor almost completely remove the aromatic compounds and organic nitriles. Therefore, the microelectrolysis reactor is an effective pre-treatment method to transform the toxic organic pollutants of ABS resin wastewater into by-products that are more biodegradable and less toxic. As a result, we can confirm that microelectrolysis reactor can be considered as a promising process for the degradation of the aromatic compounds and organic nitriles in ABS resin wastewater.

4. Conclusion

The aromatic compounds and organic nitriles in ABS resin wastewater are degraded by the microelectrolysis reactor, and their biodegradability is improved significantly. The macroscopic galvanic cells of the microelectrolysis reactor play a leading role in degradation of organic pollutants in ABS resin wastewater. The microelectrolysis reactor cannot remove the nitrogen in ABS resin wastewater, but it can transform the organic nitriles into NH_3-N, amine and acylamide, and the NH_3-N transformation efficiency reaches 50% in the influent pH 4. Moreover, the efficiency of the microelectrolysis reactor increased with the decrease of influent pH. The best value of influent pH is determined to be about 4. In this optimized condition, the COD removal efficiency is in the range of 50–55%, and the BOD_5/COD ratio is enhanced from 0.32 to 0.71 which indicates that the wastewater is biodegradable. This improvement in the biodegradability is obtained by the decomposition and transformation of the aromatic compounds and organic nitriles in ABS resin wastewater as confirmed by UV–vis, FTIR and GC–MS analysis of the treated ABS resin wastewater. This study shows that the microelectrolysis reactor can be considered as an effective, robust and economically feasible pretreatment method for ABS resin wastewater.

Acknowledgement

The research is supported by the special S&T project on treatment and control of water pollution (No. 2008ZX07207-004).

References

[1] B.Z. Qian, Market analysis on domestic and overseas ABS resin, China rubber/plast, Tech. Equip. 34 (2008) 30–37 (in Chinese).
[2] F.B. Xu, Q. Han, Global market status and prospective analysis of ABS resin, China Plast. Ind. 34 (2006) 13–25 (in Chinese).
[3] L.D. Xu, Treatment of ABS Resin Wastewater by Biological Activated Carbon Fluidized Bed, National Chung Hsing University, Taiwan, 1999, pp. 23–55 (in Chinese).
[4] T.Y. Tsai, Biodegradation of Organics and Nitrogenous Compounds in ABS Resin Manufacturing Wastewater with Denitrification and Nitrification Process, National Cheng Kung University, Taiwan, 1999, pp. 20–53 (in Chinese).
[5] S.Y. Zhou, Evaluation Technology of Bioactivity Applied in Nitrification and Denitrification Processes, National Cheng Kung University, Taiwan, 1985, pp. 22–56 (in Chinese).
[6] D.F. Zhao, H.H. Liu, G.D. Liu, Biochemical treatment technology of wastewater produced from acrylonitrile–butadiene–styrene resin, J. Univ. Pet., China (Edition of natural science) 27 (2003) 113–116.
[7] D.F. Zhao, G.D. Liu, X.N. Yi, Study on treatment of nondegradable petrochemical wastewater using modified TiO_2, J. Harb. Inst. Technol. 38 (2006) 655–660 (in Chinese).
[8] C.K. Lin, T.Y. Tsai, J.C. Liu, M.C. Chen, Enhance biodegradation of petrochemical wastewater using ozonation and bac advanced treatment system, Water Res. 35 (2001) 699–704.
[9] J.H. Sun, S.H. Shi, Y.F. Lee, S.P. Sun, Fenton oxidative decolorization of the azo dye direct Blue 15 in aqueous solution, Chem. Eng. J. 155 (2009) 680–683.
[10] X.B. Wu, X.Q. Yang, D.C. Wu, R.W. Fu, Feasibility study of using carbon aerogel as particle electrodes for edcoloration of RBRX dye solution in a three-dimensional electrode reactor, Chem. Eng. J. 138 (2008) 47–54.
[11] S.T. Kolaczkowski, P. Plucinski, F.J. Beltran, F.J. Rivas, D.B. McLurgh, Wet air oxidation: a review of process technologies and aspects in reactor design, Chem. Eng. J. 73 (1999) 143–160.
[12] H.F. Cheng, W.P. Xu, J.L. Liu, H.J. Wang, Y.Q. He, G. Chen, Pretreatment of wastewater from triazine manufacturing by coagulation, electrolysis, and internal microelectrolysis, J. Hazard. Mater. 146 (2007) 385–392.
[13] Y.P. Yang, X.H. Xu, H.F. Chen, Treatment of chitin-producing wastewater by microelectrolysis-contact oxidization, J. Zhejiang Univ. Sci. 5 (2004) 436–440.
[14] M. Kallel, C. Belaid, T. Mechichi, M. Ksibi, B. Elleuch, Removal of organic load and phenolic compounds from olive mill wastewater by Fenton oxidation with zero-valent iron, Chem. Eng. J. 150 (2009) 391–395.
[15] F. Li, J.R. Ni, Y.J. Wu, Y.Y. Zhang, Treatment of bromoamine acid wastewater using combined process of microelectrolysis and biological aerobic filter, J. Hazard. Mater. 162 (2009) 1204–1210.
[16] Y. Jin, Y. Zhang, W. Li, Experimental study on microelectrolysis technology for pharmaceutical wastewater treatment, J. Zhejiang Univ. Sci. 3 (2002) 401–404.
[17] N.C. Rao, S.V. Mohan, P. Muralikrishna, P.N. Sarma, Treatment of composite chemical wastewater by aerobic GAC-biofilm sequencing batch reactor (SBGR), J. Hazard. Mater. 124 (2005) 59–67.
[18] W.Q. Qi, Aggregative indicator and inorganic pollutant, in: F.S. Wei, W.Q. Qi (Eds.), Water and Exhausted Water Monitoring Analysis Method, China Environmental Science Press, Beijing, 2006, pp. 276–284.
[19] C. Zhou, X.H. Wen, Degradation of acid blue 45 in a white-rot fungi reactor operated under nosterile conditions, Environ. Sci. (China) 30 (2009) 235–239.
[20] S.R. Couto, E. Rosales, M.A. Sanroman, Decolourization of synthetic dyes by Trametes hirsutein expanded-bed reactors[J], Chemosphere 62 (2006) 1558–1563.
[21] W.W. Zhu, Spectra Analysis of Organic Molecular Structure, Chemical Industry Press, Beijing, 2005, pp. 6–26 (in Chinese).
[22] L. Xu, H.Z. Zhao, S.Y. Shi, G.Z. Zhang, J.R. Ni, Electrolytic treatment of C.I. acid orange 7 in aqueous solution using a three-dimensional electrode reactor, Dyes Pigments 77 (2008) 158–164.
[23] W.P. Kong, B. Wang, H.Z. Ma, L. Gu, Electrochemical treatment of anionic surfactants in synthetic wastewater with three-dimensional electrodes, J. Hazard. Mater. B137 (2006) 1532–1537.
[24] M. Pimentel, N. Oturan, M. Dezotti, M.A. Oturan, Phenol degradation by advanced electrochemical oxidation process electro-Fenton using a carbon felt cathode, Appl. Catal. B: Environ. 83 (2008) 140–149.
[25] A. Serra, X. Domenech, C. Arias, E. Brillas, J. Peral, Oxidation of α-methylphenylglycine under Fenton and electro-Fenton conditions in the dark and in the presence of solar light, Appl. Catal. B: Environ. 89 (2009) 12–21.
[26] A. Ouatmane, M.R. Provenzano, M. Hafidi, N. Senesi, Compost maturity assessment using calorimetry, spectroscopy and chemical analysis, Compost Sci. Util. 8 (2000) 135–146.
[27] Z. Droussi, V. Dorazio, M.R. Provenzano, M. Hafidi, A. Ouatmane, Study of the biodegradation and transformation of olive-mill residues during composting using FTIR spectroscopy and differential scanning calorimetry, J. Hazard. Mater. 164 (2009) 1281–1285.
[28] S. Amir, A. Jouraiphy, A. Meddich, M.E. Gharous, Structural study of humic acids during composting of activated sludge-green waste: elemental analysis, FTIR and ^{13}C NMR, J. Hazard. Mater. 177 (2010) 524–529.
[29] R. Dolphen, N. Sakkayawong, P. Thiravetyan, W. Nakbanpote, Adsorption of Reative Red 141 from wastewater onto modified chitin, J. Hazard. Mater. 145 (2007) 250–255.